

Transfer method to calibrate the normalized radiance for a CE318 Sun/sky radiometer

Kaitao Li (李凯涛)^{1,2}, Zhengqiang Li (李正强)^{1,*}, Donghui Li (李东辉)¹, Wei Li (李伟)³, Luc Blarel⁴, Philippe Goloub⁴, Torres Benjamin⁴, Hua Xu (许华)¹, Yisong Xie (谢一淞)¹, Weizhen Hou (侯伟真)¹, Li Li (李莉)¹, and Xingfeng Chen (陈兴峰)¹

¹State Environmental Protection Key Laboratory of Satellite Remote Sensing, Institute of Remote Sensing and Digital Earth, Chinese Academy of Sciences, Beijing 100101, China

²University of Chinese Academy of Sciences, Beijing 100049, China

³Hefei University of Technology, Hefei 230009, China

⁴University of Lille 1, Lille 59655, France

*Corresponding author: lizq@radi.ac.cn

Received December 22, 2014; accepted February 12, 2015; posted online March 26, 2015

A transfer method is introduced to derive the normalized radiance for CE318 Sun/sky radiometer using viewing solid angles and extraterrestrial calibration constants. The new transfer method has a good consistency at different parts of the sky scanning. Error analysis suggests that the uncertainty of the transferred method is about 2.0%–2.4%. The normalized radiances are used as input of the aerosol inversion to test the performance of the new transfer method. The residuals of the inversion (e.g., difference between fitted and measured radiance) are chosen as the index of the radiance calibration accuracy. Analyses of one year's measurements in Beijing suggest an average sky residual of 3.3% for almucantar scanning (while 3.7% for the AERONET method), which suggest a better accuracy of the transfer method when used in aerosol retrieval.

OCIS codes: 010.0280, 010.1310, 010.3920, 120.5630.

doi: 10.3788/COL201513.041001.

Ground-based radiometer observation has the highest accuracy among aerosol remote sensing approaches and can provide more inverted aerosol parameters than satellite observations. The CIMEL CE318 Sun/sky radiometer is the standard instrument^[1] used in the AERONET^[2], which consists of more than 500 observation sites all over the world. The aerosol properties provided by AERONET play an important role not only in climate change studies^[3] and environment monitoring^[4], but also in the validation of satellite aerosol products^[5]. The CE318 usually contains two kinds of measurements: spectral data of direct Sun radiation extinction and the angular distribution of sky radiances^[6]. The scattering sky radiance is the principal information used in the aerosol inversion based on remote sensing measurements^[7,8]. It can be used to retrieve aerosol properties, such as phase function, single scattering albedo, particle size distribution, and complex refractive index. The accuracies of these retrievals depend greatly on the accuracy of the sky radiance calibration^[9,10].

An integrating sphere is the primary light source for radiance calibration. However, due to limits in obtaining highly absolute accuracy of the sphere light source, at present, the radiance calibration with an uncertainty of 3%–5%^[2] is less accurate than that of the extraterrestrial radiometer constant V_0 . In terms of aerosol inversion, the sky radiance L needs to be normalized by the extraterrestrial solar irradiance E_0 . The uncertainty in E_0 can be also as large as that of L ^[11].

In order to characterize the atmospheric radiation field, CE318 measures the angular sky radiance in two parts of the sky, aureole (a) and dark-sky (k), in the almucantar (ALM) and the solar principal plane (SPP). Usually, the angular sky radiance, for the aureole part L_a , is obtained from the CE318 output digital number (DN) V_a and the radiance calibration coefficient C_a (in the units of $W/m^2/sr/nm/DN$),

$$L_a(\lambda; \Theta) = C_a \cdot V_a(\lambda; \Theta), \quad (1)$$

where λ is the central wavelength and Θ is the scattering angle. Meanwhile, according to Li *et al.*^[12], one can derive the radiance calibration coefficient as follows:

$$C_a = \frac{E_0}{\Omega_v \cdot V_0} \cdot \frac{G_s}{G_a} \cdot \frac{LG}{HG_a}, \quad (2)$$

where the solid angle Ω_v is related to the field of view (FOV) of the radiometer; V_0 denotes the radiometer signal measured at the top of the atmosphere; the subscript s refers to the instrument function using the Sun optical path; G_s and G_a are adjustable user gains for Sun and aureole measurements, respectively; LG and HG_a , respectively, represent the instrument internal gain of Sun and aureole measurements. The instrument internal gains are assumed to be independent of wavelength, when aiming at the same light source (e.g., an integrating sphere), the internal gains ratio can be expressed as

$$\frac{LG}{HG_a} = \frac{V_s(\lambda)}{V_a(\lambda)} \cdot \frac{G_a(\lambda)}{G_s(\lambda)}. \quad (3)$$

Then, applying Eqs. (2) to the angular sky radiance [Eq. (1)], we obtain,

$$L_a(\lambda; \Theta) = \frac{LG \cdot G_s(\lambda) \cdot E_0(\lambda)}{\Omega_v \cdot HG_a \cdot G_a(\lambda) \cdot V_0(\lambda)} \cdot V_a(\lambda; \Theta). \quad (4)$$

The downward normalized sky radiance L' is defined as follows:

$$L'(\lambda; \Theta) = \frac{\pi \cdot L(\lambda; \Theta)}{E_0(\lambda) \cdot f_{es}}, \quad (5)$$

where f_{es} means the Earth-Sun distance correction factor corresponding to the sky radiance acquisition time. Combining Eqs. (4) and (5), the normalized sky radiance can be yielded as

$$L'_a(\lambda; \Theta) = \frac{\pi \cdot LG \cdot G_s(\lambda)}{\Omega_v \cdot HG_a \cdot G_a(\lambda) \cdot V_0(\lambda) \cdot f_{es}} \cdot V_a(\lambda; \Theta). \quad (6)$$

Based on the double 6° sky measurement (D6sky), part of the CE318 observation protocol that consists of sequential aureole and dark-sky radiance measurements at a fixed scanning angle (6°) within a very short time period (<1 s)^[12], when aiming at the same light source, the relationship between the aureole and dark-sky measurements can be described as

$$C_k(\lambda) = C_a(\lambda) V_a^{\textcircled{6}}(\lambda) / V_k^{\textcircled{6}}(\lambda), \quad (7)$$

where C_k is the dark-sky radiance calibration coefficient $V_a^{\textcircled{6}}$ and $V_k^{\textcircled{6}}$ are output DNs of the aureole and dark-sky measurements at the scanning angle of 6°. Then the dark-sky normalized radiance L_k can be expressed as

$$L'_k(\lambda; \Theta) = \frac{\pi \cdot LG \cdot G_s(\lambda)}{\Omega_v \cdot HG_a \cdot G_a(\lambda) \cdot V_0(\lambda) \cdot f_{es}} \cdot \frac{V_a^{\textcircled{6}}}{V_k^{\textcircled{6}}} \cdot V_k(\lambda; \Theta). \quad (8)$$

Equations (6) and (8) provide a method to transfer the instrument extraterrestrial constant V_0 and the viewing solid angle Ω_v to the normalized sky radiance L' by measuring radiometer output signals in the field.

A CIMEL CE318 Sun/sky radiometer, number 350 in AERONET^[2], located on the roof of the Institute of Remote Sensing and Digital Earth (RADI), was used in this research work. The type of the radiometer #350 is dual Polar (DP), which has ten channels centered at 340, 380, 440, 500, 675, 870, 936, 1020, 1020i, and 1640 nm. The spectral channel 1020i is the second 1020 nm band using an independent optical path shared with the 1640 nm band^[2,13], thus radiometer #350 is characterized by two viewing solid angles and two FOVs (one is covering the spectral range 340–1020 nm, and the other is covering the channels of 1020i and 1640 nm. In this Letter, the normalized radiances of six SKY measurement channels for two geometries are considered, while the bands used in the inversion procedures are only four common channels for the ALM measurement geometry.

The extraterrestrial constant V_0 of radiometer #350 is obtained by comparing with a master radiometer at Carpentras, a field calibration site located in southeastern France, on November 2, 2009, and the radiance calibration coefficients are obtained with an integrating sphere in Lille, France on October 28, 2009. The calibration coefficients are listed in Table 1.

The viewing solid angle Ω_v (units of sr) is a function of the FOV,

$$\Omega_v = 2\pi(1 - \cos(\text{FOV}/2)). \quad (9)$$

The FOV is a basic parameter of an optical instrument, usually fixed in the design and manufacture (nominally 1.2° for the new CE318 radiometer types, e.g., NE, DP). However, this angle may change with instruments produced in different periods and especially with different types of instruments. According to Torres *et al.*^[14], the maximum discrepancy of the FOV with respect to the CIMEL specification (1.2°) was 10%.

There are two ways to derive this solid angle. One is the so-called vicarious method by which one can directly compute this solid angle from historical calibration coefficients by using Eq. (2); the specific calculation steps have been presented by Li *et al.*^[12], and the solid angle calculated from Eq. (2) is 4.0268×10^{-4} sr for 340–1020 nm channels and 4.0114×10^{-4} sr for 1640 and 1020i nm bands, and the FOVs are 1.297° and 1.295°, respectively, following Eq. (9).

Alternatively, by geometrically measuring the FOV of the radiometer, one can compute the solid angle by using

Table 1. Calibration Coefficients of Radiometer #350 on November 2, 2009 and October 28, 2009

WV (nm)	1020	1640	870	675	440	500
V_0	9885.2	11303.8	26820.2	18751.1	10868.4	14905.4
C_a (W/m ² /sr/nm/DN)	0.01802	0.00247	0.01708	0.01954	0.03956	0.03104
C_k (W/m ² /sr/nm/DN)	0.00225	0.00031	0.00427	0.00488	0.00988	0.00776
E_0 (W/m ² /nm)	0.70776	0.23273	0.95432	1.51577	1.84143	1.92228

Eq. (9). A matrix measurement method^[14,15] (the program to control the radiometer to do matrix measurements is provided by Cimel Electronique) was used to compute the FOV of the radiometer. The calculation of the Ω_v is given in^[14]

$$\Omega_v = \sum_{x,y} \frac{V(x,y)\Delta S}{V(x_c,y_c)}, \quad (10)$$

where x and y are the orthogonal coordinates, $V(x,y)$ represents the DN measured at coordinate (x,y) , x_c and y_c are the estimated pointing errors; ΔS is the differential area, same as $dx dy$.

In this Letter, the matrix measurement in the lab by using laser as light source was chosen to obtain the FOVs of radiometer #350 on August 20, 2014 at 03:00:00 (UTC). The subfigure on the left in Fig. 1 displays the 3D surface map of the raw measurements. The right subfigure shows the plane map of the measurements. The average FOV calculated from five matrix measurements is $1.300^\circ (\pm 0.004^\circ)$ for 340–1020 nm, which is close to the results of the vicarious method.

In this Letter, the FOV obtained with matrix measurements of the laser was adopted to calculate the normalized radiance.

The extraterrestrial solar irradiance at each wavelength is calculated from the convolution of the solar spectral irradiance and the filter transmittance (the response function of the sensor is flat within the narrow band according to the manufacture), as follows:

$$E_0(\lambda) = \frac{\int_{\lambda_1}^{\lambda_2} E_s(\lambda) \cdot R(\lambda) \cdot d\lambda}{\int_{\lambda_1}^{\lambda_2} R(\lambda) \cdot d\lambda}, \quad (11)$$

where $E_s(\lambda)$ is the spectral irradiance of the Sun, $R(\lambda)$ is the spectral transmittance profile of the filter from the instrument manufacturer, and λ_1 and λ_2 denote the boundaries of the filter profile. In this work, we consider using the ASTM2000 spectra^[16], which has been

commonly used in the community. The spectral irradiance of #350, $E_0(\lambda)$, can be found in Table 1.

According to the D6sky measurement protocol of the CE318 radiometer, the aureole and dark-sky measurements at the fixed scanning angle, 6° , should be the same, ignoring the time shift of the two measurements and the errors during the optical signal to electrical signal conversion of the radiometer. However, there is always some discrepancy of radiances at 6° due to the uncertainties of the radiance calibration coefficients following traditional AERONET's calibration approach. In order to explain this discrepancy, we first employ one year's (2010) measurements to calculate the normalized radiance with AERONET calibration coefficients C_a and C_k , and then we compare the radiances of the D6sky measurements. Two examples, measured in SPP and ALM measurement geometries, have been chosen to illustrate the jump between aureole and dark-sky measurements at the scanning angle of 6° . Table 2 shows the differences in the normalized radiance based on AERONET calibration between D6sky measurements for SPP and ALM geometries, while the radiance calculated with the new transfer method is exactly the same.

AERONET's inversion code^[9] was chosen to test the performance of the aerosol retrievals. The normalized radiances calculated with AERONET calibration coefficients C_a , C_k and the transfer method are chosen as the input. Meanwhile, the AOD and other initial guesses are kept the same for the two inversion procedures. Therefore, differences can only originate from the two calibration approaches to investigate the performance of the transfer method.

One year's measurements by radiometer #350 at the Beijing RADi in 2010 were analyzed in this Letter. The average radiance difference at the scanning angle of 6° is 0.79% for ALM measurement geometry with the AERONET calibration. During the inversion procedure, the total residuals are 3.7% and 4.1% (the sky part residuals are 3.3% and 3.7%) by using the transfer method and the AERONET calibrations, respectively, according

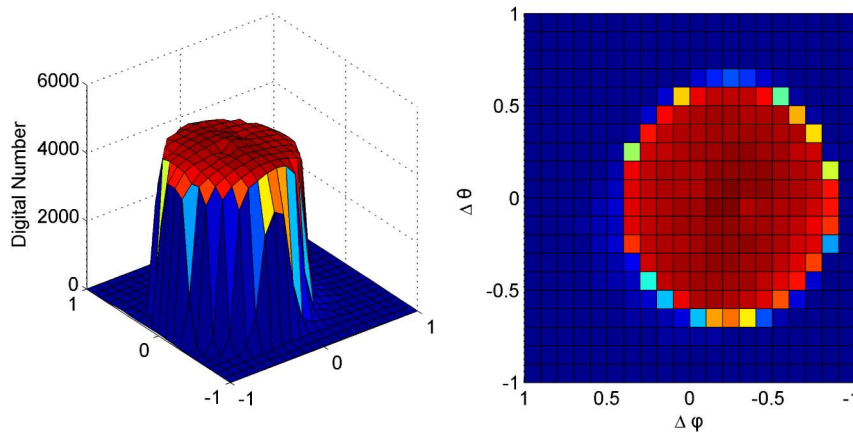


Fig. 1. Matrix measurements of radiometer #350. The left one shows the 3D surface map of the raw measurements taken in Beijing on August 20, 2014 at 03:00:00 (UTC), while the right one shows the plane map of the measurements.

Table 2. Average Differences in Normalized Radiance L' Based on AERONET Calibration Between Double 6° Sky Measurements for Radiometer #350 in the Year 2010

WV (nm)	1020	1640	870	675	440	500
Diff. in SPP L' (%)	0.32	0.28	0.19	0.27	0.15	0.18
Diff. in ALM L' (%)	0.52	0.50	0.54	0.57	0.21	0.55

to residual definitions in AERONET's quality assurance criteria^[17].

Figure 2 shows one year of average residuals of normalized sky radiances based on fitted and measured normalized radiance corresponding to the AERONET calibrations and the transfer method in ALM geometry. The residuals of the transfer method is generally smaller than that of the AERONET. Figure 3 shows an example of retrievals based on the AERONET calibrations and the transfer method. The total residuals (consisting of Sun and sky parts) of the inversion are 2.6% and 2.8% for the transfer method and the AERONET calibrations, respectively. There are differences in these two retrievals. From the previous

$$\frac{\Delta L'_a}{L'_a} = \sqrt{\left(\frac{\Delta \Omega_v}{\Omega_v}\right)^2 + \left(\frac{\Delta(f_{es})}{f_{es}}\right)^2 + \left(\frac{\Delta\left(\frac{LG}{HG_a}\right)}{\frac{LG}{HG_a}}\right)^2 + \left(\frac{\Delta\left(\frac{G_s}{G_a}\right)}{\frac{G_s}{G_a}}\right)^2 + \left(\frac{\Delta V_0}{V_0}\right)^2 + \left(\frac{\Delta V_a}{V_a}\right)^2}. \quad (12)$$

description, the better retrievals come from the more accurate normalized radiances, thus the retrievals from the transfer method seem better than the AERONET method although there are no true values of the retrievals.

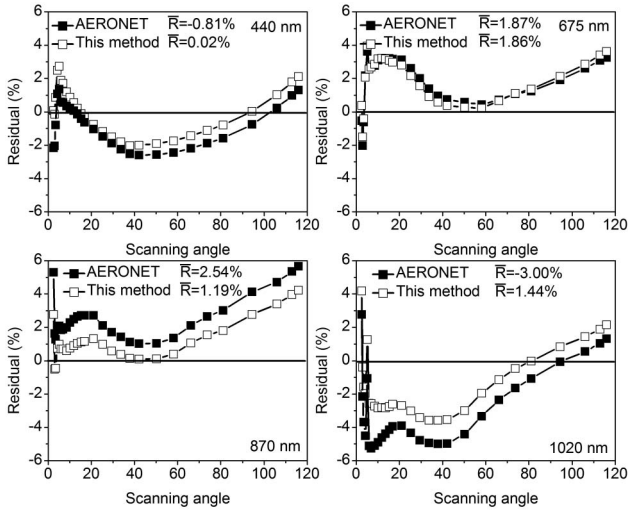


Fig. 2. Comparison of one year's averaged inversion residuals (difference between the fitted and measured normalized radiance) corresponding to the AERONET calibrations and the transfer method in ALM geometry; \bar{R} denotes the averaged residual of the inversion.

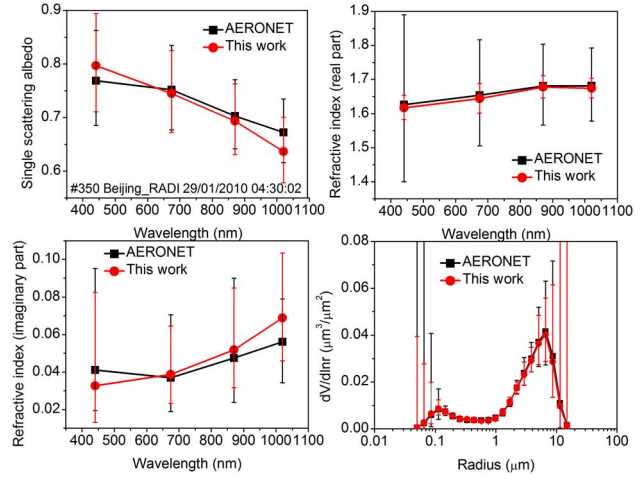


Fig. 3. Comparison of retrievals corresponding to the AERONET calibrations and the transfer method in ALM geometry. The vertical lines mean the min and max values of the retrievals.

The uncertainties in normalized radiance L' can be estimated by the error propagation following Eq. (6); considering the independent error sources, one can obtain

On the right hand side of Eq. (12), four items are important: (i) the instrument viewing solid angle Ω_v ; (ii) the internal gain ratios LG/HG_a ; (iii) the instrument calibration coefficient V_0 ; (iv) the instrument measurement V_a . The uncertainty of the Sun-Earth distance correction factor is 10^{-4} ^[18], which can be ignored considering it is minor compared with other error sources. The uncertainties from user gain ratios, the G items, can also be neglected considering the gain techniques employed by the modern radiometers are sufficiently precise^[13]. The estimated uncertainties are listed in Table 3.

Table 3. Uncertainties Estimated on the Normalized Radiance Based on the Transfer Method

Error sources	Uncertainties (%)
$\Delta \Omega_v / \Omega_v$	1.5
$\Delta\left(\frac{LG}{HG_a}\right) / \frac{LG}{HG_a}$	0.5
$\Delta V_0 / V_0$ (master, field)	0.5, 1.5
$\Delta V_a / V_a$	0.5
Others	0.5
Total	2.0 (master)/2.4(field)

The most important error sources are from the viewing solid angle Ω_v and V_0 . The uncertainty in Ω_v obtained by using the vicarious method is $\sim 1.5\%$ according to Li *et al.*^[13], while the estimated error in Ω_v obtained from the matrix measurement is also $\sim 1.5\%$ and can be decreased in the future. The uncertainty in V_0 for the Langley calibration instrument is $\sim 0.5\%$ ^[2] and, for the field calibration, one must consider an extra $\sim 1\%$ error in V_0 ^[2]. The error in LG/HG_a is from electronic circuit resistances, which have an order of magnitude of $\sim 0.5\%$ compared to theoretical values^[12]. The error on the output DN has an uncertainty of $\sim 0.5\%$. The uncertainty in “others” covers all possible remaining error sources, e. g., errors in the user gain ratio items, the dark signal correction, and the spectral variation of the Ω_v due to the optical dispersion effect. According to Eq. (12), the final uncertainty of L is $\sim 2.0\%$ for the Langley calibrated instruments, $\sim 2.4\%$ for the field calibrated instruments depending on V_0 .

In conclusion, we propose a new transfer method to derive the normalized radiance for the ground-based CE318 Sun/sky radiometer. We present two methods to obtain the viewing solid angle Ω_v , which is then combined with the radiometer extraterrestrial constant V_0 to calculate the normalized radiance. The matrix measurement is done in the lab on August 20, 2014, which has a FOV of 1.300° for 340–1020 nm. The accuracy of the normalized radiance is assessed based on the error propagation method, which are $\sim 2.0\%$ for the Langley calibrated instruments and $\sim 2.4\%$ for the field calibrated instruments, depending on V_0 . The consistency of the double 6° sky measurements is inspected, and the residuals of the aerosol inversion are compared. The new transfer method possesses the following features: (i) it avoids using $E_0(\lambda)$, which has considerable uncertainty; (ii) the transfer method uses high precision V_0 instead of C_a and C_k . At the same time, considering the joint constraint of the AOD and radiance during the inversion, this transfer method guarantees the consistency of the input information and inversion process, hence can improve the accuracy of retrievals; (iii) the transfer method is easy to use and it does not need to do any integrating sphere calibration in the lab. Moreover, this method can be further improved by considering Ω_v wavelength dependence, and more accurate Ω_v characterization approaches.

This work was supported by the Research Equipment Development Project of the Chinese Academy of Sciences (No. YZ201224), the National Natural Science Foundation of China (No. 41222007), the Chinesisch-Deutsches

Forschungsprojekt (No. GZ659), and the Key Project of the Scientific and Technological Innovation of the Chinese Academy of Sciences (No. KGFZD-125-13-006). The authors thank the AERONET team at Carpentras and LOA for helping to do the field and radiance calibrations used in this study. We are grateful to Oleg Dubovik of LOA for the inversion algorithm. We also thank Marius Canini (Cimel Electronique) for providing the matrix measurement program.

References

1. M. Xia, J. Li, Z. Li, D. Gao, W. Pang, D. Li, and X. Zheng, *Chin. Opt. Lett.* **12**, 121201 (2014).
2. B. N. Holben, T. F. Eck, I. Slutsker, D. Tanré, J. P. Buis, A. Setzer, E. Vermote, J. A. Reagan, Y. J. Kaufman, T. Nakajima, F. Lavenu, I. Jankowiak, and A. Smirnov, *Remote Sens. Environ.* **66**, 1 (1998).
3. S. Solomon, D. Qin, M. Manning, M. Marquis, K. Averyt, M. M. B. Tignor, H. L. Miller, and Z. Chen, *The Physical Science Basis. Contribution of Working Group I to the Fourth Assessment Report of the Intergovernmental Panel on Climate Change* (Cambridge University, 2007).
4. I. Colbeck and M. Lazaridis, *Naturwissenschaften* **97**, 117 (2010).
5. Q. Xu, Z. Obradovic, B. Han, Y. Li, A. Braverman, and S. Vucetic, in *Proceeding of the 8th International Conference on Information Fusion* 654 (2005).
6. O. Dubovik, A. Smirnov, B. N. Holben, M. D. King, Y. J. Kaufman, T. F. Eck, and I. Slutsker, *J. Geophys. Res.* **105**, 9791 (2000).
7. X. Sun and H. Wang, *Chin. Opt. Lett.* **12**, 012901 (2014).
8. K. Yan, S. Wang, S. Jiang, L. Xue, Y. Song, Z. Yan, and Z. Li, *Chin. Opt. Lett.* **12**, 092901 (2014).
9. O. Dubovik and M. D. King, *J. Geophys. Res.* **105**, 20673 (2000).
10. B. Torres, O. Dubovik, C. Toledano, A. Berjon, V. E. Cachorro, T. Lapyonok, P. Litvinov, and P. Goloub, *Atmos. Chem. Phys.* **14**, 847 (2014).
11. C. Wehrli, *Metrologia* **37**, 419 (2000).
12. Z. Li, L. Blarel, T. Podvin, P. Goloub, J.-P. Buis, and J.-P. Morel, *Appl. Opt.* **47**, 1368 (2008).
13. Z. Li, P. Goloub, L. Blarel, B. Yang, K. Li, T. Podvin, D. Li, Y. Xie, X. Chen, X. Gu, X. Zheng, J. Li, and M. Catalfamo, *Appl. Opt.* **52**, 2226 (2013).
14. B. Torres, C. Toledano, A. Berjon, D. Fuertes, V. Molina, R. Gonzalez, M. Canini, V. E. Cachorro, P. Goloub, T. Podvin, L. Blarel, O. Dubovik, Y. Bennouna, and A. M. de Frutos, *Atmos. Meas. Tech.* **6**, 2207 (2013).
15. T. Nakajima, G. Tonna, R. Rao, P. Boi, Y. Kaufman, and B. Holben, *Appl. Opt.* **35**, 2672 (1996).
16. “2000 ASTM Standard Extraterrestrial Spectrum Reference E-490-00,” <http://rredc.nrel.gov/solar/spectra/am0/ASTM2000.html>.
17. B. N. Holben, T. F. Eck, I. Slutsker, A. Smirnov, A. Sinyuk, J. Schafer, D. Giles, and O. Dubovik, *Proc. SPIE* **6408**, 64080Q (2006).
18. K. N. Liou, *An Introduction to Atmospheric Radiation*, 2nd ed. (Academic, 2002).